

# Reactivity of a platinum $\eta^1$ -formylketenyl complex Synthesis of a platinum $\alpha$ -pyrone derivative via generation and trapping of a $C_3H_2O_2$ species. 20\*

Luciano Pandolfo, Gastone Paiaro\*\* and Paolo Ganis†

Dipartimento di Chimica Inorganica, Metallorganica e Analitica, Univ. di Padova, via Marzolo 1, I-35134 Padua (Italy)

Giovanni Valle

CNR, Centro di Studio sui Biopolimeri, via Marzolo 1, I-35134 Padua (Italy)

Pietro Traldi

CNR, Area di Ricerca di Padova, Corso Stati Uniti 4, I-35100 Padua (Italy)

(Received February 1, 1993; revised March 19, 1993)

## Abstract

The formylketenyl platinum complex, *trans*-bis(tricyclohexylphosphine)( $\eta^1$ -formylketenyl)(hydride)platinum(II), *trans*-(PCy<sub>3</sub>)<sub>2</sub>(H)Pt[ $\eta^1$ -C(CHO)CO] (**1**), reacts with acids causing the cleavage of the Pt–C bond and generating the species C<sub>3</sub>H<sub>2</sub>O<sub>2</sub> which is trapped by an excess of **1**. The reaction gives rise to the formation of the addition product *trans*-(PCy<sub>3</sub>)<sub>2</sub>(H)Pt(C<sub>6</sub>H<sub>3</sub>O<sub>4</sub>), where C<sub>6</sub>H<sub>3</sub>O<sub>4</sub> is an  $\alpha$ -pyrone ligand  $\sigma$ -bonded to Pt. The crystal structure of the Pt  $\alpha$ -pyrone derivative has been determined. The crystals are monoclinic, space group *P2*<sub>1</sub>/*a*, with *a* = 19.404(9), *b* = 11.889(6), *c* = 18.534(9),  $\beta$  = 91.3(1)°, *Z* = 4. The plane of the  $\alpha$ -pyrone ligand is almost orthogonal to the coordination plane of Pt. IR, <sup>1</sup>H and <sup>31</sup>P NMR and mass spectra also support the structure.

## Introduction

The chemistry of ketenes, as well as that of related metal complexes, has been receiving increasing attention and has been extensively reviewed [2]. Of relevant interest are studies concerning the tautomeric equilibrium ketene/ynol [3], the reactivity of ketenes and acyl ketenes [2a, 4] and the synthesis and reactivity of metal ketenyl complexes [5, 6]. Moreover, vinylketene complexes are postulated as intermediates in reactions leading to a variety of organic cyclic compounds [7].

The bis-ketene carbon suboxide, C<sub>3</sub>O<sub>2</sub>, has also been the subject of intensive study, with the aim to discover and explain its reactivity toward metal compounds [1]. It yields, through simple reactions, ketene, ketenyls and ketenylidene metal complexes [6, 8].

In the course of our study we synthesized the formylketenyl platinum derivative *trans*-bis(tricyclohexylphosphine)( $\eta^1$ -formylketenyl)(hydride)platinum(II), *trans*-(PCy<sub>3</sub>)<sub>2</sub>(H)Pt[ $\eta^1$ -C(CHO)CO] (**1**) [6b] (Fig.

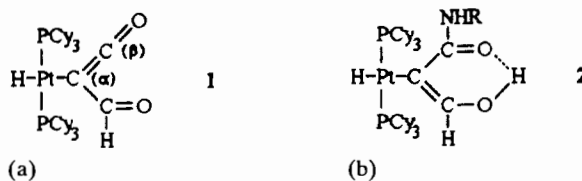


Fig. 1. Schematic structure of *trans*-(PCy<sub>3</sub>)<sub>2</sub>(H)Pt[ $\eta^1$ -C(CHO)CO] (a) and of its enolic-amidic derivative (b).

**1**(a)). Its reactivity is quite different from that presented by ketenyls so far known; it rather resembles that of organic acylketenes [4].

For instance, metal ketenyls, as well as ketenes, add HNu to the olefinic double bond [2c, 5a], whereas the addition of amines to **1** gives the enolic-amidic derivative **2** (Fig. 1(b)), which presents a hydrogen-bridged six-membered ring [6d]. Such behaviour has also been found in the reaction of **1** with H<sub>2</sub>O or ROH [9], and is similar to that shown by acylketenes in the reaction with H<sub>2</sub>O, ROH or amines [4b, c].

The acylketenes are highly reactive intermediates and are, as a rule, prepared and used *in situ* by thermal decomposition of appropriate diazo compounds [4b, c] or 1,3-dioxinones [4d]. On the contrary **1** is a stable

\*For Part 19, see ref. 1.

\*\*Author to whom correspondence should be addressed.

†On sabbatical leave from University of Napoli, Italy.

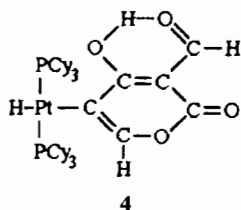


Fig. 2. Schematic structure of *trans*-(PCy<sub>3</sub>)<sub>2</sub>(H)Pt(C<sub>6</sub>H<sub>3</sub>O<sub>4</sub>).

metal-substituted formylketene and can be used as a suitable model to investigate the reactivity of acylketenes.

To this purpose, we treated **1** with an equimolecular amount of HCl, obtaining the unexpected facile cleavage of the Pt–C<sub>α</sub> bond and the formation of the species C<sub>3</sub>H<sub>2</sub>O<sub>2</sub> (**3**) which has been detected by mass spectrometry in the reaction system [10], but could not be isolated, owing to its high reactivity.

Here we report the behaviour of **1** when reacted with organic acids in a ratio Pt:RCOOH = 2:1. In the first step of the reaction, **3** is produced and then it is trapped by the excess of **1** yielding the platinum  $\alpha$ -pyrone compound **4** (Fig. 2). Details of the reaction, physico-chemical characterization and the X-ray structure of **4** are reported.

## Experimental

### General comments

All reactions and manipulations were carried out under an atmosphere of dry argon with standard Schlenk, vacuum line or septum/cannula techniques. Glassware was oven-dried prior to use. Solvents were purified, dried and distilled before use. The formylketenyl complex **1** was synthesized as previously described [6b].

IR spectra were obtained on a Perkin-Elmer 597 spectrophotometer. <sup>1</sup>H and <sup>31</sup>P NMR spectra were recorded on a Varian EM 360A or on a JEOL FX 900 instrument and chemical shifts are reported in  $\delta$  relative to TMS and to 85% H<sub>3</sub>PO<sub>4</sub>, respectively. Elemental analyses were provided by the Microanalysis Laboratory of the CIMA Department of the University of Padova. Mass spectra were obtained by a VG ZAB2F (VG Analytical, UK) instrument operating in FAB conditions. The nitrobenzyl alcohol solutions of the samples were bombarded by 8 KeV Xe atoms.

### Synthesis of (PCy<sub>3</sub>)<sub>2</sub>(H)Pt(C<sub>6</sub>H<sub>3</sub>O<sub>4</sub>) (**4**)

The formylketenyl complex **1** (0.880 g, 1.07 mmol) was dissolved at 40 °C in 10 ml of toluene and 0.065 g (0.535 mmol) of PhCOOH, dissolved in 5 ml of toluene, was slowly added to the stirred solution. After 10 min a yellow solid began to precipitate. The sus-

pension was cooled at –20 °C, filtered and the solid, washed with cold toluene and dried under vacuum, analysed as **4**·toluene. Yield 0.410 g (77%). The solid was recrystallized from CHCl<sub>3</sub>/n-heptane by slow evaporation, giving light yellow, well-formed crystals of **4**. Mother liquors were concentrated to 3 ml and cooled at –40 °C. A yellow cream solid precipitated; it was filtered and dried under vacuum. Yield 0.400 g. From elemental analysis and NMR spectra it was recognized as *trans*-(PCy<sub>3</sub>)<sub>2</sub>(H)Pt(PhCOO) (**5**).

**4**: m.p. 214–217 °C (dec.). IR (CH<sub>2</sub>Cl<sub>2</sub>):  $\nu$ (C–H) 2930–2850,  $\nu$ (Pt–H) 2043,  $\nu$ (COO) 1716–1692,  $\nu$ (CO) 1617 cm<sup>-1</sup>. <sup>1</sup>H NMR (CDCl<sub>3</sub>, 28 °C,  $\delta$ ): 14.27 (s, OH), 10.01 (s, CHO), 6.95 (s,  $J(^{195}\text{Pt}-^1\text{H})=34.2$  Hz, =CH), 1.78–1.16 (complex pattern, C<sub>6</sub>H<sub>11</sub>), –8.68 (t,  $J(^{31}\text{P}-^1\text{H})=15.38$  Hz,  $J(^{195}\text{Pt}-^1\text{H})=692.14$  Hz, Pt–H). <sup>31</sup>P NMR (CDCl<sub>3</sub>, 28 °C,  $\delta$ ): 35.34 (s,  $J(^{195}\text{Pt}-^{31}\text{P})=2744.16$  Hz). *Anal.* Calc. for PtC<sub>42</sub>H<sub>70</sub>O<sub>4</sub>P<sub>2</sub>: C, 56.26; H, 7.87. Found: C, 56.70; H, 8.06%

**4**·C<sub>7</sub>H<sub>8</sub>: *Anal.* Calc. for PtC<sub>49</sub>H<sub>78</sub>O<sub>4</sub>P<sub>2</sub>: C, 59.55; H, 7.95. Found: C, 58.94; H, 7.58%

**5**: <sup>1</sup>H NMR (CDCl<sub>3</sub>, 28 °C,  $\delta$ ): 1.91–1.08 (complex pattern, C<sub>6</sub>H<sub>11</sub>), –22.85 (t,  $J(^{31}\text{P}-^1\text{H})=14.1$  Hz,  $J(^{195}\text{Pt}-^1\text{H})=1341$  Hz, Pt–H). <sup>31</sup>P NMR (CDCl<sub>3</sub>, 28 °C,  $\delta$ ): 40.97 (s,  $J(^{195}\text{Pt}-^{31}\text{P})=2908.2$  Hz). *Anal.* Calc. for PtC<sub>43</sub>H<sub>72</sub>O<sub>4</sub>P<sub>2</sub>: C, 58.82; H, 8.26. Found: C, 58.64; H, 8.01%.

Similar results were obtained when **1** was reacted with MeCOOH in 2:1 ratio.

The FAB mass spectrum of **4** shows a well detectable molecular ion at  $m/z$  894 (related to <sup>194</sup>Pt). The base peak is due to PtH(PCy<sub>3</sub>)<sub>2</sub><sup>+</sup> at  $m/z$  755 and further ions at  $m/z$  672, 589, 506 originate from the ion at  $m/z$  755 through sequential losses of Cy.

When **1** is reacted with PhCOOH in 1:1 ratio only **5** was (nearly quantitatively) obtained, with a little quantity of a red solid that was not identified (see 'Results and discussion').

### X-ray data collection

Crystals of **4**, suitable for X-ray analysis were obtained by recrystallization from CHCl<sub>3</sub>/heptane. A single crystal was mounted on a Philips-PW1100 computer-controlled four-circle diffractometer with graphite monochromator. Standard centring and autoindexing procedures indicated the primitive monoclinic lattice  $P2_1/a$ . The orientation matrix and accurate unit cell dimensions were determined from a least-square fit of 25 symmetry related reflections. Intensity data were collected at 25 °C using the  $\theta$ – $2\theta$  scan method; two standard reflections, monitored every 150 reflection measurements, fluctuated within  $\pm 2\%$  of their mean value. The intensities were corrected for Lorentz and polarization effects and for minor absorption effects by empirical ( $\psi$ -scan) meth-

ods ( $\mu=31\text{ cm}^{-1}$ ). Crystal data and details of data collection are reported in Table 1.

### Solution and refinement of the structure

The positions of Pt and P were determined from a tridimensional Patterson synthesis. The light atoms were located from subsequent Fourier maps. Most of the hydrogen atoms were located from the last difference synthesis; yet, they have been geometrically recalculated, assigned isotropic thermal parameters (with  $U(\text{H})=1.2U_{\text{eq}}(\text{C})$  or  $1.2U_{\text{eq}}(\text{O})$ ) and included in the final calculations, but not refined.

Anisotropic thermal parameters were used for all the non-hydrogen atoms. Blocked-cascade least-square refinements were used: they converged to the conventional  $R$  index of 0.037. A unitary weighting scheme was used. Scattering factors for the atoms were taken from Cromer and Waber [11]; the scattering factors for Pt and P were corrected for the real and imaginary parts of anomalous dispersion by using Cromer's values [12]. All computations were carried out on a Cyber-76 computer using the programs of ref. 13. The final positional parameters of the non-hydrogen atoms are listed in Table 2. See also 'Supplementary material'.

TABLE 1. Crystal data and details of intensity measurements for **4**

Formula	PtC <sub>42</sub> H <sub>70</sub> O <sub>4</sub> P <sub>2</sub>
Formula weight	896.05
Space group	$P2_1/a$
Cell constants	
<i>a</i> (Å)	19.404(9)
<i>b</i> (Å)	11.889(6)
<i>c</i> (Å)	18.534(9)
$\beta$ (°)	91.3(1)
Cell volume (Å <sup>3</sup> )	4274.58
<i>Z</i>	4
$D_{\text{calc}}$ (g cm <sup>-3</sup> )	1.39
Radiation	graphite monochromatized Mo K $\alpha$ (0.7107 Å)
Crystal size (mm)	0.15 × 0.12 × 0.15
<i>T</i> (K)	298
$\mu$ (cm <sup>-1</sup> )	30.97
Absorption correction	empirical methods ( $\psi$ -scan)
Diffractionmeter	Philips PW 1100
Take off angle (°)	3
2 $\theta$ Range (°)	3.0 ≤ 2 $\theta$ ≤ 45
Scan mode	$\theta$ -2 $\theta$
No. collected reflections	7536
No. reflections with $I \geq 3\sigma(I)$	4707
<i>R</i>	0.037
$R_w$	0.039
<i>GOF</i>	1.273
$\Delta(\rho)$ (e Å <sup>-3</sup> )	0.51

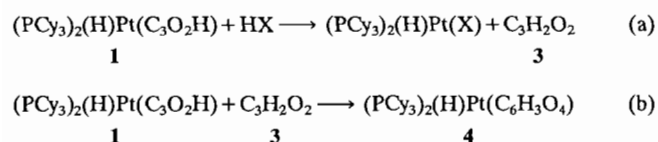
TABLE 2. Final fractional atomic coordinates of the non-hydrogen atoms for **4**

Atom	<i>x</i>	<i>y</i>	<i>z</i>
Pt	0.27349(2)	0.57456(3)	0.75976(2)
P(1)	0.3563(1)	0.4819(2)	0.6969(1)
P(2)	0.2158(1)	0.6938(2)	0.8335(1)
O(1)	0.1407(4)	0.5881(6)	0.6504(4)
O(2)	0.0386(6)	0.524(1)	0.5734(7)
O(3)	0.1385(5)	0.2755(8)	0.7389(5)
O(4)	0.0505(5)	0.2228(8)	0.6729(7)
C(1)	0.1925(6)	0.461(1)	0.7297(6)
C(2)	0.1883(5)	0.3533(7)	0.7587(5)
C(3)	0.0876(6)	0.301(1)	0.6852(7)
C(4)	0.0909(6)	0.408(1)	0.6576(7)
C(5)	0.1404(5)	0.485(1)	0.6793(6)
C(6)	0.036(1)	0.431(1)	0.6041(9)
C(7)	0.3252(4)	0.3761(8)	0.6307(5)
C(8)	0.2859(5)	0.4378(9)	0.5666(5)
C(9)	0.2488(6)	0.342(1)	0.5185(6)
C(10)	0.2993(6)	0.253(1)	0.4934(7)
C(11)	0.3393(6)	0.200(1)	0.5546(6)
C(12)	0.3756(5)	0.2856(8)	0.6048(5)
C(13)	0.4158(4)	0.4026(8)	0.7582(5)
C(14)	0.3737(5)	0.3173(8)	0.8018(5)
C(15)	0.4213(7)	0.251(1)	0.8525(7)
C(16)	0.4609(7)	0.327(1)	0.9041(7)
C(17)	0.5037(6)	0.410(1)	0.8595(7)
C(18)	0.4565(5)	0.4813(9)	0.8095(5)
C(19)	0.4121(4)	0.5858(7)	0.6532(5)
C(20)	0.4715(4)	0.5342(8)	0.6087(5)
C(21)	0.5212(5)	0.627(1)	0.5853(6)
C(22)	0.4815(6)	0.717(1)	0.5422(6)
C(23)	0.4238(5)	0.7675(9)	0.5863(6)
C(24)	0.3732(5)	0.6747(8)	0.6102(5)
C(25)	0.1231(4)	0.6641(7)	0.8457(5)
C(26)	0.1121(5)	0.5535(8)	0.8853(5)
C(27)	0.0374(6)	0.517(1)	0.8788(7)
C(28)	-0.0106(6)	0.607(1)	0.9081(7)
C(29)	0.0005(6)	0.718(1)	0.8699(8)
C(30)	0.0758(5)	0.7544(9)	0.8759(6)
C(31)	0.2168(5)	0.8410(8)	0.7998(5)
C(32)	0.2892(6)	0.8914(9)	0.7972(7)
C(33)	0.2850(8)	1.012(1)	0.7688(8)
C(34)	0.248(1)	1.019(1)	0.6977(9)
C(35)	0.1756(9)	0.970(1)	0.6995(8)
C(36)	0.1775(7)	0.850(1)	0.7268(7)
C(37)	0.2603(5)	0.7012(8)	0.9230(5)
C(38)	0.2351(6)	0.7834(9)	0.9774(5)
C(39)	0.2821(8)	0.795(1)	1.0426(6)
C(40)	0.3146(8)	0.697(1)	1.0692(6)
C(41)	0.3382(6)	0.611(1)	1.0147(6)
C(42)	0.2868(8)	0.598(1)	0.9520(6)

### Results and discussion

When HX (X = Cl, RCOO) is rapidly added to **1** in 1:1 ratio, only *trans*-(PCy<sub>3</sub>)<sub>2</sub>(H)Pt(X) is recovered and **3** is detected only by mass spectrometry [10]. If the reaction is carried out with slow addition of acid and, above all, in a 2:1 ratio, the excess of **1** is able to trap

**3** giving **4**. The comprehensive process can be summarized by the two reactions of Scheme 1.



Scheme 1.

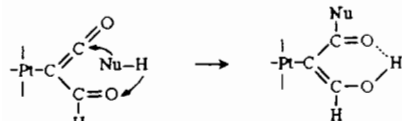
Following the pathway proposed for acylketenes [4c, d], Scheme 2 can explain the reactivity of **1** toward HNu, in agreement with the electronic charges as calculated for formylketene [14].

When Nu is NHR the product is stable and **2** is obtained [6d]. If Nu is OH or OR, analogous compounds are formed in equilibrium with reagents [9].

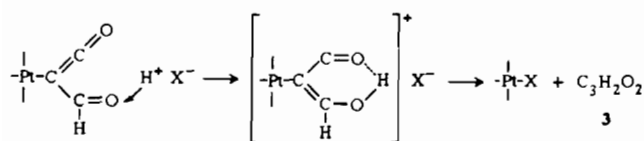
If **1** is reacted with HX (X = Cl [10] or RCOO) the course of the reaction is ruled by the formation of an unstable cation (Scheme 3) which decomposes with cleavage of the Pt–C bond, formation of Pt–X and of the species **3**, which can be described in terms of the tautomeric equilibria of Scheme 4.

The second step of the reaction is the trapping of **3**, if an excess of **1** is present, to give **4**. On the basis of our results it is not possible to define univocally the mechanism of the addition of **3** to the formylketenyl moiety of **1** and, in particular, to specify if **3** reacts as the tautomeric form formyl ynol or as a ketene. The presence of the formyl ynol **3a** in the reaction system, when **1** is reacted with acids, was proved by a MIKE spectrum of the ionic species at  $m/z$  70 [10], but a composite peak at  $m/z$  41 and AMNDO calculations [10] also support the possible existence of isomers **3b** and **3c**.

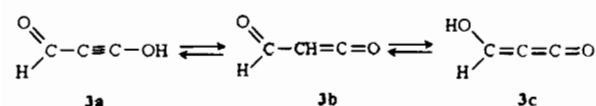
As regards the trapping of **3**, it is to point out that the reaction of **1** with the forms **a**, **b** or **c** can generate



Scheme 2.



Scheme 3.



Scheme 4.

**4** anyhow. Moreover it is to note that acylketenes can react with enol ethers giving  $\alpha$ -pyrones [4a] and can dimerize yielding dehydroacetic acid [4d] with a [4 + 2] cycloaddition. A similar behaviour is observed in reactions of vinylketene complexes with alkynes [7c], and likely the same mechanism applies to the reaction (1b), leading to the formation of the  $\alpha$ -pyrone ligand  $\sigma$ -bonded to Pt.

The red solid, scarcely soluble in most organic solvents, obtained when **1** reacts with acids in 1:1 ratio (see 'Experimental'), is likely a polymer derived from the highly reactive compound **3**.

The X-ray structural analysis confirms the  $\alpha$ -pyronic constitution of **4**.

The most relevant geometrical parameters of this complex are reported in Table 3 and the molecular structure is shown in Fig. 3.

All the atoms of the  $\alpha$ -pyronic ligand lie almost exactly on a plane (see Table 4).

The bond lengths in the six-membered ring (C(1)–C(2)–O(3)–C(3)–C(4)–C(5)) range between 1.36(2) and 1.39(2) Å (except for C(3)–O(3) = 1.42(2) Å), which approaches a resonant system.

The coplanarity of the residue O(1)–C(5)–C(4)–C(6)–O(2) with the  $\alpha$ -pyronic ring is accomplished through a hydrogen bridge between O(1) and O(2), which fact justifies the short interatomic distance O(1)···O(2) of 2.55 Å. The bridging hydrogen between the two oxygen atoms could not be located on difference

TABLE 3. Selected bond distances (Å) and bond angles (°) with e.s.d.s. for **4**

Bond distances			
Pt–P(1)	2.288(3)	C(1)–C(2)	1.39(2)
Pt–P(2)	2.281(3)	C(2)–O(3)	1.38(1)
Pt–C(1)	2.14(1)	O(3)–C(3)	1.42(2)
P(1)–C(7)	1.849(9)	C(3)–C(4)	1.37(2)
P(1)–C(13)	1.859(9)	C(4)–C(5)	1.39(2)
P(1)–C(19)	1.843(9)	C(1)–C(5)	1.39(2)
P(2)–C(25)	1.852(8)	C(3)–O(4)	1.20(2)
P(2)–C(31)	1.860(9)	C(4)–C(6)	1.47(2)
P(2)–C(37)	1.850(9)	C(5)–O(1)	1.33(1)
		C(6)–O(2)	1.25(2)
Bond angles			
P(1)–Pt–P(2)	195.4(2)	C(3)–C(4)–C(5)	123.0(9)
P(1)–Pt–C(1)	94.9(3)	C(4)–C(5)–C(1)	123.0(9)
P(2)–Pt–C(1)	100.1(3)	C(5)–C(1)–C(2)	114.0(9)
Pt–P(1)–C(7)	116.3(4)	O(3)–C(3)–O(4)	112.0(9)
Pt–P(1)–C(13)	111.5(3)	C(4)–C(3)–O(4)	133.0(9)
Pt–P(1)–C(19)	109.1(3)	C(3)–C(4)–C(6)	113.0(9)
Pt–P(2)–C(25)	116.5(3)	C(5)–C(4)–C(6)	124.0(8)
Pt–P(2)–C(31)	112.0(3)	C(4)–C(6)–O(2)	116.0(8)
Pt–P(2)–C(37)	109.9(3)	C(4)–C(5)–O(1)	120.0(9)
Pt–C(1)–C(2)	122.0(8)	C(1)–C(5)–C(4)	123.0(9)
C(1)–C(2)–O(3)	124.1(9)	C(1)–C(5)–O(1)	117.0(8)
C(2)–O(3)–C(3)	121.1(9)	C(4)–C(5)–O(1)	120.0(8)
O(3)–C(3)–C(4)	115.0(9)	C(5)–C(1)–Pt	124.2(7)

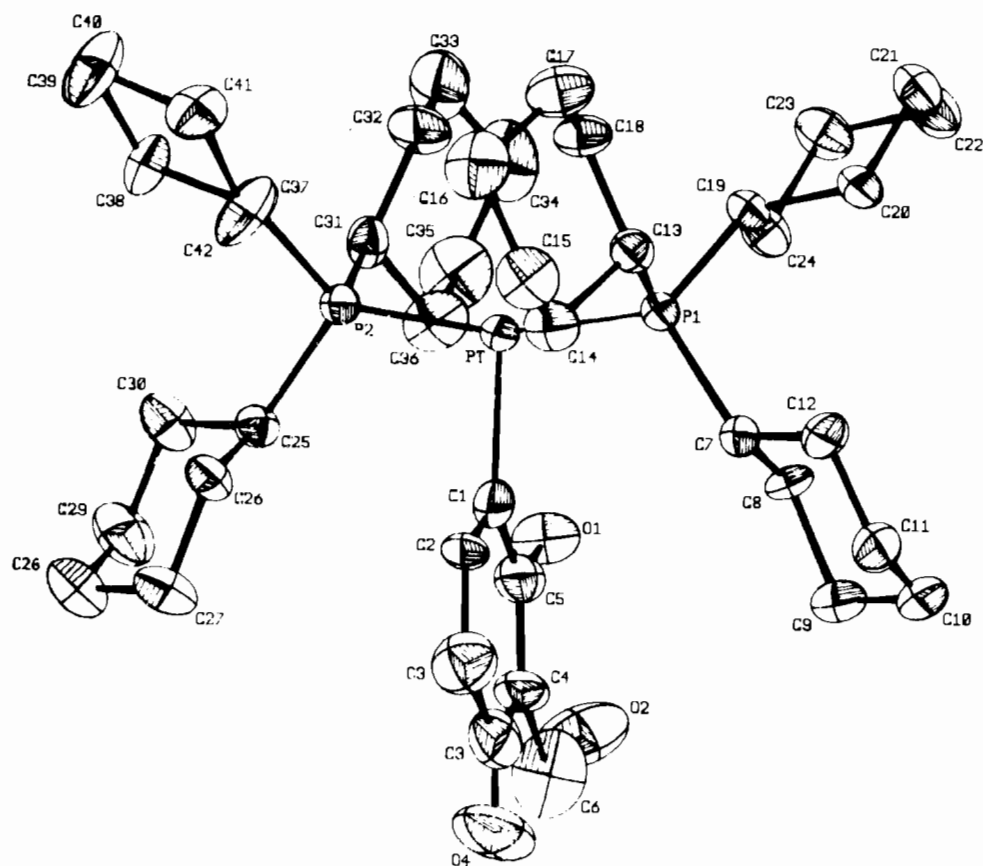


Fig. 3. ORTEP diagram of **4** with the labelling scheme for the non-hydrogen atoms.

TABLE 4. Equations of the least-square planes with distances (Å) of the atoms from planes given in brackets

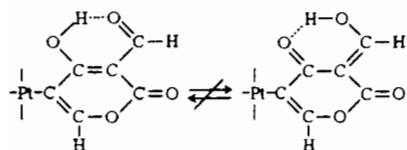
$\alpha$  Plane C(1), C(2), C(3), C(4), C(5), C(6), O(1), O(2), O(3), O(4)  $0.6202x - 0.3270y - 0.7130z = -9.3406$   
 [C(1) 0.033, C(2) 0.010, C(3)  $-0.008$ , C(4)  $-0.009$ , C(5)  $-0.009$ , C(6) 0.041, O(1)  $-0.015$ , O(2) 0.041, O(3)  $-0.019$ , O(4) 0.017]

$\beta$  Plane P(1), P(2), Pt, C(1)  $-0.162x + 0.6042y - 0.7802z = -7.6683$   
 [P(1)  $-0.016$ , P(2)  $-0.018$ , Pt 0.005, C(1)  $-0.100$ ]

Dihedral angle  $\alpha\beta = 75.0^\circ$

Fourier syntheses; nonetheless its position has been calculated geometrically and assigned to the enolic oxygen O(1). The bond lengths C(5)–O(1) (1.33(2) Å) and C(6)–O(2) (1.25(2) Å) are in full accordance with the values expected for enolic and aldehydic C–O bonds, respectively [15]. Therefore, no tautomerism of the type shown in Scheme 5 seems to be present in this structure.

The molecule exhibits a pseudo- $C_2$  symmetry with the twofold axis passing through the Pt–C(1) bond (see



Scheme 5.

Fig. 3). The coordination of Pt is slightly distorted square planar. The angle P(1)–Pt–P(2) of *c.*  $195^\circ$  is imposed by the intramolecular non-bonded interaction between the  $\alpha$ -pyronic ligand and cyclohexyl groups. The hydrogen atom bonded to Pt has not been located; its expected position is coincident with ripples around the heavy atom.

As found in all the Pt  $\alpha$ -alkenyl complexes related to carbene derivatives [16, 17], the plane of the  $\alpha$ -pyronic ligand nearly bisects the angle P–Pt–P and is almost orthogonal to the coordination plane of Pt. Here the deviation from orthogonality is *c.*  $15^\circ$  (see Table 4). No particular explanation can be attached to this deviation except for intramolecular steric effects. In Table 5 are reported some significant intramolecular distances which account for this conformational pa-

TABLE 5. Some significant intramolecular non-bonded distances (Å) between the  $\alpha$ -pyronic group and the closest cyclohexyl rings

O(1)···C(8)	3.70	O(1)···C(25)	3.75
C(2)···C(7)	3.61	C(2)···C(26)	3.67
C(5)···C(8)	3.59	C(5)···C(25)	3.76
O(1)···C(36)	3.48	C(5)···C(26)	3.95
C(2)···C(14)	3.69		

parameter. Due to the same reasons the bond angles Pt–P(1)–C(7) and Pt–P(2)–C(25) are widened to *c.* 116°.

All the other geometrical parameters are quite normal and do not require particular comments, see ‘Supplementary material’.

IR and NMR spectra show that the main features of **4** are retained also in solution. The singlet at 35.34 ppm in the <sup>31</sup>P NMR spectrum is quite normal for two tricyclohexylphosphines *trans* bonded to Pt. The <sup>1</sup>H NMR spectrum shows four significant signals attributable to the enolic-bridged OH (singlet at 14.27 ppm which disappears by shaking with D<sub>2</sub>O), to the aldehydic hydrogen (singlet at 10.01 ppm), to the vinylic hydrogen (singlet at 6.95 ppm with Pt satellites) and to Pt–H (triplet at –8.68 ppm, which is in accordance with a Pt-bonded hydride *trans* to a C atom). The presence of the signal attributable to the aldehydic hydrogen and its integration ratio of 1:1 with the other three significant hydrogen signals exclude, at least at r.t., the existence of the tautomerism of Scheme 5.

The intense absorption at 2930–2850 cm<sup>–1</sup>, ascribable to  $\nu$ (C–H) of cyclohexyl, likely covers the signal due to the enolic OH, lowered by an intramolecular hydrogen bond. Shaking of a CH<sub>2</sub>Cl<sub>2</sub> solution of **4** with D<sub>2</sub>O gives rise to the broadening of the Pt–H signal (2043 cm<sup>–1</sup>), to which the signal due to the O–D stretching is probably superimposed, according to a value of  $\nu$ (OH) near 2800–2900 cm<sup>–1</sup>. This fact, with the concomitant low value of the aldehydic CO stretching (1617 cm<sup>–1</sup>), comparable with the corresponding value for salicylaldehyde (1637 cm<sup>–1</sup>), supports the existence of a hydrogen bridge between O(1) and O(2).

Signals at 2043 and 1692 cm<sup>–1</sup>, attributable to Pt–H and pyronic COO, respectively, are in accordance with the proposed structure.

The mass spectrometric behaviour of **4** fully agrees with the above findings. A well detectable molecular ion is present at *m/z* 894 (related to <sup>194</sup>Pt) together with fragment ions related to the reported structure (see ‘Experimental’). The primary loss of the whole pyrone moiety, leading to the fragment ion at *m/z* 755 is observed. In the low mass region an intense peak at *m/z* 70 is detected, for which both accurate mass measurements and daughter ion spectroscopy indicate the possible structure of formyl ynol [10]. Parent ion scan, performed on this ion, does not show the presence

of any precursor, so suggesting its origin from a thermal process.

## Conclusions

The reactions reported here confirm the peculiar reactivity of the formylketenyl platinum complex **1**.

The unexpectedly facile cleavage of the Pt–C bond by treatment with HCl [10] and the formation of **3** are also found by reacting **1** with weak acids.

On the one hand the reactivity of **1** resembles the one shown by Mo and W  $\eta^2$ -ketenyl complexes in the preparation of transition metal coordinated ynols [18]. On the other hand **1** can be considered as a metal-substituted formylketene, and presents the typical reactivity of acylketenes, thus allowing the trapping of **3** in compound **4**. It is important to emphasize that **3** can be released from **4**, as shown by mass spectrometry experiments, which enables this elusive compound to be isolated.

It is also worth noting that obtaining an  $\alpha$ -pyrone, with formation of C–C and C–O bonds, suggests that **1** is in some ways reminiscent of carbon suboxide, from which it is derived. In fact, C<sub>3</sub>O<sub>2</sub> easily produces  $\alpha$ -pyrones by reacting with  $\beta$ -diketones or phenols [19] and polymerizes yielding poly  $\alpha$ - and  $\gamma$ -pyrones [20].

The behaviour of **1** with acids confirms the stabilizing effect of Pt bonded to the central carbon atom on the, otherwise, highly reactive formyl ketene. Therefore the usefulness of **1** as a stable model for investigating the reactivity of acylketenes is ascertained.

The presence in **4** of the enolic form of a  $\beta$ -dicarbonyl moiety (H–O(1)–C(5)–C(4)–C(6)–O(2)), similar to that exhibited by **2**, enables **4**, **2** and other similar compounds, as sophisticated analogues of  $\beta$ -diketones, to be used in the synthesis of some bimetallic derivatives. This last point is, at present, the subject of our investigations.

## Supplementary material

Tables of thermal parameters of the non-hydrogen atoms, positional parameters of hydrogen atoms, bond angles and bond distances (4 pages) and a list of observed and calculated structure factors (27 pages) for **4** are available from the authors on request.

## Acknowledgements

This work was supported by MURST (40%) (Roma) and by the Consiglio Nazionale delle Ricerche (CNR, Roma). We are indebted to Mr G. Ravazzolo for technical assistance.

## References

- 1 G. Paiaro and L. Pandolfo, *Comments Inorg. Chem.*, **12** (1991) 213.
- 2 (a) H.R. Seikaly and T.T. Tidwell, *Tetrahedron*, **42** (1986) 2587; (b) T.T. Tidwell, *Acc. Chem. Res.*, **23** (1990) 1973; (c) G.L. Geoffroy and G.L. Bassner, *Adv. Organomet. Chem.*, **28** (1988) 1.
- 3 (a) R. Hochstrasser and J. Wirz, *Angew. Chem., Int. Ed. Engl.*, **29** (1990) 411; (b) A.J. Kresge, *Acc. Chem. Res.*, **23** (1990) 43.
- 4 (a) R.S. Coleman and E.B. Grant, *Tetrahedron Lett.*, **31** (1990) 3677; (b) H. Meier, H. Wengeroth, W. Lauer and W. Vogt, *Chem. Ber.*, **121** (1988) 1643; (c) H. Meier, H. Wengeroth, W. Lauer and V. Krause, *Tetrahedron Lett.*, **31** (1989) 5253; (d) R.J. Clemens and J.S. Witzeman, *J. Am. Chem. Soc.*, **111** (1989) 2186, and refs. therein.
- 5 (a) K. Eberl, M. Wolfgruber, W. Siebert and F.R. Kreissl, *J. Organomet. Chem.*, **236** (1982) 171; (b) F.R. Kreissl, G. Reber and G. Muller, *Angew. Chem., Int. Ed. Engl.*, **25** (1986) 643, and refs. therein.
- 6 (a) G.L. Hillhouse, *J. Am. Chem. Soc.*, **107** (1985) 7772; (b) L. Pandolfo and G. Paiaro, *Gazz. Chim. Ital.*, **120** (1990) 531; (c) P. Ganis, G. Paiaro, L. Pandolfo and G. Valle, *Gazz. Chim. Ital.*, **120** (1990) 541; (d) G. Paiaro, L. Pandolfo, P. Ganis and G. Valle, *Organometallics*, **10** (1991) 1527.
- 7 (a) K.H. Dotz, *Angew. Chem., Int. Ed. Engl.*, **23** (1981) 587; (b) S.H. Cho and L.S. Liebeskind, *J. Org. Chem.*, **52** (1987) 2631; (c) M.A. Huffmann and L.S. Liebeskind, *J. Am. Chem. Soc.*, **112** (1990) 8617.
- 8 (a) G. Paiaro and L. Pandolfo, *Angew. Chem., Int. Ed. Engl.*, **20** (1981) 288; (b) L. Pandolfo, G. Paiaro, G. Valle and P. Ganis, *Gazz. Chim. Ital.*, **115** (1985) 59; (c) G. Paiaro and L. Pandolfo, *Angew. Chem., Int. Ed. Engl.*, **20** (1981) 289.
- 9 L. Pandolfo, unpublished results.
- 10 L. Pandolfo, G. Paiaro, A. Somogy, S. Catinella and P. Traldi, *Rapid Commun. Mass Spectrom.*, **7** (1993) 132.
- 11 D.T. Cromer and J.T. Waber, *Acta Crystallogr.*, **18** (1965) 184.
- 12 D.T. Cromer, *Acta Crystallogr.*, **18** (1965) 17.
- 13 G.M. Sheldrick, *SHELX-76*, Program for crystal structure determination, Cambridge University, UK, 1976.
- 14 L. Gong, M.A. McAllister and T.T. Tidwell, *J. Am. Chem. Soc.*, **113** (1991) 6021.
- 15 *International Tables for X-ray Crystallography*, Reidel, Boston, MA, 1983.
- 16 F.R. Hartley, in G. Wilkinson (ed.), *Comprehensive Organometallic Chemistry*, Vol. 6, Pergamon, Oxford, 1982, pp. 509, 536, 539.
- 17 P.L. Bellon, M. Manassero, F. Porta and M. Sansoni, *J. Organomet. Chem.*, **80** (1974) 139.
- 18 (a) J.B. Sheridan, G.L. Geoffroy and A.L. Rheingold, *Organometallics*, **5** (1986) 1514; (b) K.A. Belsky, M.F. Asaro, S.Y. Chen and A. Mayr, *Organometallics*, **11** (1992) 1926.
- 19 T. Kappe and E. Ziegler, *Angew. Chem., Int. Ed. Engl.*, **13** (1974) 491.
- 20 T. Carofiglio, L. Pandolfo and G. Paiaro, *Eur. Polym. J.*, **22** (1986) 491.